hydroxyl, etc.) on the electrode surfaces.[26]

The value of k_q evaluated in this work can be used to help distinguish among the various schemes considered by Rubinstein and Bard in discussing the potential dependence of the electrochemiluminescence they observed when $Ru(bpy)_3^{2+}$ in Nafion films was oxidized to $Ru(bpy)_3^{3+}$ in the presence of oxalate anions.[6] The digital simulation procedure they employed produced acceptable fits of the experimental data for three alternative sets of rate constants for several of the key reactions, so that an unambiguous mechanistic assignment was not possible. The values of k_q producing the three best fits were 0, 5×10^7, and 2×10^9 $M^{-1}\ s^{-1}$. The second is closest to the values measured in these experiments, and this prompts us to assign the mechanistic scheme that corresponds to this value in the digital simulation of ref 6 as the correct one. One consequence of this assignment is that the $Ru(bpy)_3^{2+*}$ generated in the experiments of Rubinstein and Bard[6] must have arisen from the reduction of $Ru(bpy)_3^{3+}$ by both CO_2^- and $Ru(bpy)_3^+$.

Conclusions

The spectroelectrochemical procedure employed here to measure the concentrations of $Ru(bpy)_3^{2+}$ and $Ru(bpy)_3^{3+}$ in Nafion films on transparent tin oxide electrodes is reliable and especially useful in cases where redox couples that do not adhere to the Nernst equation are under study. The use of polymer films on electrodes to house emitting and quenching species in Stern–Volmer experiments is attractive because the concentration of quencher can be varied continuously by control of the electrode potential. In favorable cases, data for an entire Stern–Volmer plot can be obtained in a single experiment. The example presented in these experiments involved the quenching of the luminescence from one half of a redox couple by the other half of the same couple, but the procedure is also applicable to cases in which the quenching is by an independent redox couple (Figure 9).

The results of luminescence quenching experiments proved useful in probing the structures of Nafion films as the earlier work of Lee and Meisel[17] suggested they might be. The experiments indicate that cast Nafion films have more homogeneous structures than bulk membranes of Nafion. They also show that significant changes in the local polyelectrolyte environment accompany the oxidation of $Ru(bpy)_3^{2+}$ to $Ru(bpy)_3^{3+}$ in Nafion films. The magnitude of the quenching rate constant measured in the Nafion films allows a choice to be made among possible mechanistic schemes proposed previously[6] for the generation of electrochemiluminescence at Nafion-coated electrodes.

Acknowledgment. Special thanks are due Daniel Nocera and Jay Winkler for assistance with the photochemical experiments and their interpretation. We acknowledge with gratitude the receipt of preprints from Professor A. J. Bard and co-workers and additional helpful discussions with them. This work was supported by the U.S. Army Research Office.

Registry No. $Ru(bpy)_3^{3+}$, 18955-01-6; $Ru(bpy)_3^{2+}$, 15158-62-0; Nafion, 39464-59-0; oxalate, 144-62-7.

---

[26] Vaughan, R. J., private communication, 1981.

Intramolecular Potential Functions from Observed Crystal Structures. 1. 1,3,5-Triphenylbenzene, *p*,*p*′-Bitolyl, 1,1′-Binaphthyl, and *o*-Terphenyl[1]

William R. Busing

Contribution from the Chemistry Division, Oak Ridge National Laboratory,
Oak Ridge, Tennessee 37830. *Received January 11, 1982*

Abstract: The crystal structures of the title compounds were reproduced by minimizing the energies of computational models with respect to lattice parameters, molecular rotations and translations, and the intramolecular torsion angles between rigid phenyl or naphthyl groups. The energies of the models were calculated by using potential functions that include terms for intermolecular and intramolecular nonbonded interactions and a conjugation energy or π-bonding term that is a function of the phenyl–phenyl or naphthyl–naphthyl torsion angles. The values of these angles computed for the crystals were shown to depend on the coefficients of the latter terms, and these coefficients were adjusted to reproduce the experimental torsion angles as well as possible. The adjusted values obtained for the four compounds are similar but not identical, and they are bracketed by various values reported from theoretical calculations on biphenyl. *o*-Terphenyl was represented by a more complicated model, which allows for bond-angle and out-of-plane distortions of the phenyl–phenyl bonds. Potential energy curves and equilibrium conformations were calculated for the isolated molecules. Four published nonbonded potentials for hydrocarbons were tested, and a 6–exp–1 function was selected as best for this work.

The conformation of a molecule in the crystalline state differs from that of the isolated molecule because of effects that may be attributed to intermolecular forces. For small molecules, such forces are now very well-known,[2] and even for large molecules, they have been fairly well characterized. For hydrocarbons, for example, potentials have been developed that are able to reproduce the observed crystal structures, heats of sublimation, and external vibrational frequencies to a good approximation.[3-10]

Intramolecular potentials, on the other hand, have been used extensively for predicting the conformations and energies of isolated molecules.[11-13] Most of these potentials have been designed

---

[1] Research sponsored by the Division of Materials Sciences, Office of Basic Energy Sciences, U.S. Department of Energy, under Contract W-7405-eng-26 with the Union Carbide Corp.

[2] For a review, see: Barker, J. A.; Henderson, D. *Rev. Mod. Phys.* **1976**, *48*, 587–671.

[3] Kitaigorodsky, A. I.; Mirskaya, K. V. *Sov. Phys.-Crystallogr.* (*Engl. Transl.*) **1964**, *9*, 137–142.

[4] Warshel, A.; Lifson, S. *J. Chem. Phys.* **1970**, *53*, 582–594.

[5] Taddei, G.; Bonadeo, H.; Marzocchi, M. P.; Califano, S. *J. Chem. Phys.* **1973**, *58*, 966–978.

[6] Mirskaya, K. V.; Kozlova, I. E.; Bereznitskaya, V. F. *Phys. Status Solidi B* **1974**, *62*, 291–294.

[7] Momany, F. A.; Carruthers, L. M.; McGuire, R. F.; Scheraga, H. A. *J. Phys. Chem.* **1974**, *78*, 1595–1620.

[8] Taddei, G.; Righini, R.; Manzelli, P. *Acta Crystallogr., Sect. A* **1977**, *A33*, 626–628.

[9] Williams, D. E.; Starr, T. L. *Comput. Chem.* **1977**, *1*, 173–177.

[10] Mirsky, K. In "Computing in Crystallography"; Schenk, H., Olthof-Hazekamp, R., van Koningsveld, H., Bassi, G. C., Eds.; Delft University Press: Delft, The Netherlands, 1978; pp 169–182.

0002-7863/82/1504-4829$01.25/0

Table I. 1,3,5-Triphenylbenzene: Observed and Calculated Crystal Structure Parameters and Calculated Geometry of the Idealized Isolated Molecule[a,b]

	crystal				isolated molecule
	obsd[23]	calcd	calcd − obsd	%	calcd
a	7.61	7.39	−0.22	−2.9	
b	19.76	19.80	0.04	0.2	
c	11.26	11.20	−0.06	−0.5	
x^c	0.00	0.03	0.03		
θ^d	0.0	0.6	0.6		
ϕ_1	−39.2	−38.1	1.1		43.6
ϕ_2	35.9	36.5	0.6		43.6
ϕ_3	−34.8	−35.2	−0.4		43.6

[a] E_ϕ = 8.68 kcal/mol. [b] Lengths are in angstroms; angles in degrees. [c] Overall molecular translation (angstroms). [d] Overall molecular rotation (degrees).

to reproduce known molecular geometries, thermochemical properties, and vibrational frequencies. For large molecules, however, the gas-phase conformations are not always well-known and the vibrational spectra may not be easy to analyze.

In this paper we will concern ourselves initially with the torsion potential about a phenyl–phenyl bond and the contribution that conjugation makes to it. Several theoretical calculations of this potential have been made,[14–17] but the approximations are usually severe for such large molecules. In pioneering work in 1972, Williams[18] showed that the phenyl–phenyl torsion potential in *p,p′*-bitolyl could be derived by modeling the crystal structure using combined intra- and intermolecular potential functions. The purpose of the present effort is to extend this work to several compounds in a way that is generally similar to but that differs in detail from the technique used by Williams. We propose to demonstrate that in favorable cases, when observed crystal structures are available that show molecules distorted significantly either by intermolecular packing forces or by intramolecular nonbonded interactions and when these nonbonded forces can be assumed known, then the other constants that define the intramolecular potential can be determined.[19]

1,3,5-Triphenylbenzene. This compound provides a straightforward example of the procedure we will follow. The experimental crystal structure[23] is known to be orthorhombic (space group $Pna2_1$) with four symmetrically equivalent molecules in the unit cell. Table I lists some of the parameters of the structure, and a single molecule is illustrated in Figure 1. No symmetry is imposed on this molecule by the crystalline environment, and the sign of one of the three phenyl–phenyl torsion angles differs from that of the other two, an accident of the optimum packing arrangement. Of more interest to use are the differences of from 1 to 4° in the observed magnitudes of the three torsion angles ϕ_1, ϕ_2, and ϕ_3 (39.2, 35.9, and 34.8°, respectively). Each of these values is the average of the four conformation angles (or their negative supplements) about a phenyl–phenyl bond. Thus, ϕ_1 is the average of torsion angles 2–1–7–12 and 6–1–7–8 with the negative supplements of angles 2–1–7–8 and 6–1–7–12. This convention, which is used throughout the paper, is needed because these angles are generally not exactly equal for distorted molecules.

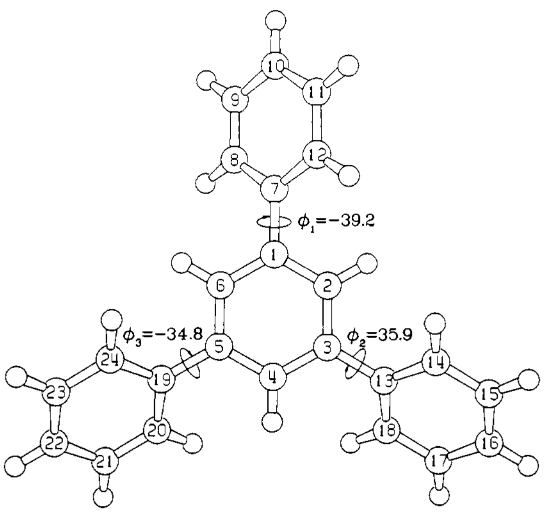

Figure 1. Molecular geometry of 1,3,5-triphenylbenzene as observed in the crystal structure. Each angle shown is the average of four conformation angles (degrees) as described in the text.

We will construct a computational model of the crystal structure and minimize its energy. Each benzene ring with its hydrogen atoms will be taken as a rigid segment with the carbon atoms having the geometry found by X-ray diffraction. The hydrogen atoms are placed in computed positions on a line extending from the center of the ring (the mean of the carbon positions) through a carbon atom to give a constant C–H distance chosen as described below. Each phenyl group is allowed to pivot with one degree of freedom about the ring–ring bond (hereafter called a "link"). The entire molecule is permitted to orient itself with three degrees of rotational freedom and to translate in the crystal *x* and *y* directions with two degrees of freedom. Translation in the *z* direction is irrelevant in this polar space group. The three lattice parameters *a*, *b*, and *c* of the orthorhombic cell are the final variables of our model, making a total of 11 degrees of freedom. In all adjustments of these variables, we maintain the crystal symmetry, so that any changes in the position or conformation of the basic molecule are repeated for all molecules in the crystal. For some special purposes, it may be desirable to relax these symmetry constraints and to increase the number of variables, but in the present calculations, this would only increase the computing time while producing the same results.

To complete our model, we need to define a potential so that the energy of the system can be calculated as a function of the geometry. For nonbonded interactions, we select the atom–atom potential of Williams and Starr[9], a 6–exp–1 potential of the form

$$V(r) = -A_{ij}r^{-6} + B_{ij}\exp(-C_{ij}r) + q_iq_jr^{-1} \qquad (1)$$

where *r* is the interatomic distance, the coefficients A_{ij}, B_{ij}, and C_{ij} depend on the kinds of atoms involved, and the q_i's are Coulomb charges assigned to the various kinds of atoms. In the Appendix we will tabulate the coefficients of this potential together with those of three alternative ones, and we will report the results of tests that justify our selection of the Williams and Starr potential.

Equation 1 is used to compute a contribution from each nonbonded interaction, both intermolecular and intramolecular. Terms corresponding to nonbonded contacts within the same rigid group are not included since these remain constant. Interactions between geminal atoms (atoms bonded to the same atom) are also omitted. These terms are constant for the present model but not for the more general model used for *o*-terphenyl later.

---

(11) Ermer, O.; Lifson, S. *J. Am. Chem. Soc.* **1973**, *95*, 4121–4132.

(12) Engler, E. M.; Andose, J. D.; Schleyer, P. v. R. *J. Am. Chem. Soc.* **1973**, *95*, 8005–8025.

(13) Wertz, D. H.; Allinger, N. L. *Tetrahedron* **1979**, *35*, 3–12.

(14) Fischer-Hjalmars, I. *Tetrahedron* **1963**, *19*, 1805–1815.

(15) Casalone, G.; Mariani, C.; Mugnoli, A.; Simonetta, M. *Mol. Phys.* **1968**, *15*, 339–348.

(16) Dewar, M. J. S.; Harget, A. J. *Proc. R. Soc. London, Ser. A* **1970**, *315*, 443–455.

(17) Almlöf, J. *Chem. Phys.* **1974**, *6*, 135–139.

(18) Williams, D. E. *Acta Crystallogr., Sect A* **1972**, *A28*, 629–635.

(19) Extensive work has been done on biphenyl itself[15,20] in an effort to reconcile the apparent large difference between its conformations in the gas and crystalline phases. It appears that there is still some uncertainty as to whether the room-temperature crystal is an ordered or disordered structure,[20,21] and we regard this as a case that is unfavorable for the present kind of analysis. Recently, an ordered low-temperature modification of biphenyl with nonplanar molecules has been studied;[22] modeling of this structure may be possible.

(20) Brock, C. P. *Mol. Cryst. Liq. Cryst.* **1979**, *52*, 157–162.

(21) Charbonneau, G. P.; Delugeard, Y. *Acta Crystallogr., Sect. B* **1976**, *B32*, 1420–1423.

(22) Cailleau, H.; Baudour, J. L.; Zeyen, C. M. E. *Acta Crystallogr., Sect. B* **1979**, *B35*, 426–432.

(23) Lin, Y. C.; Williams, D. E. *Acta Crystallogr., Sect. B* **1975**, *B31*, 318–320.

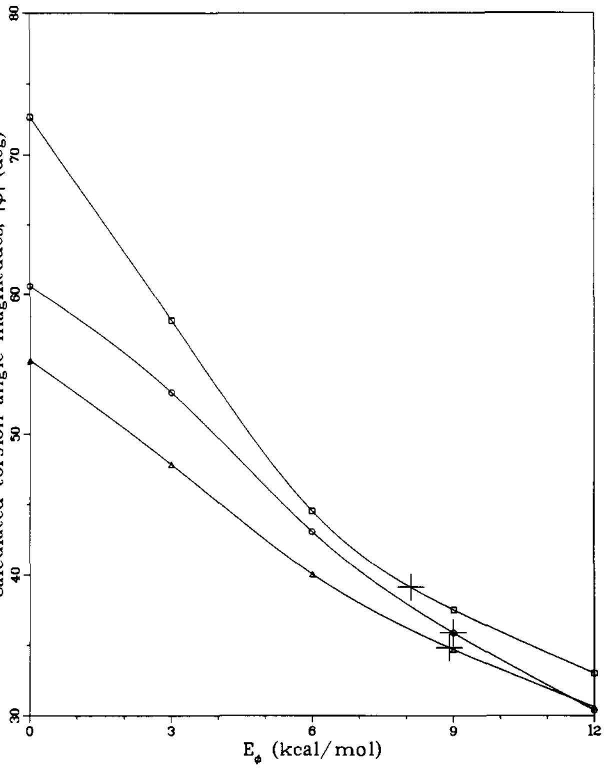

Figure 2. Magnitudes of the three phenyl-phenyl torsion angles of 1,3,5-triphenylbenzene obtained by minimizing the energy of a computational model of the crystal using various values of the π-bonding potential parameter E_ϕ. The + signs indicate the observed values of these angles.

Williams and Starr assume that their interactions involving hydrogen atoms are centered at a point on the C–H bond 0.07 Å from the H nucleus. For this reason, we have set our calculated H positions 1.020 Å from C rather than at the accepted C–H distance of 1.090 Å.

We represent the π-bonding interactions, which arise from the partial double-bond character of the links and which tend to make the rings coplanar, by an expression of the form

$$V(\phi) = (E_\phi/4)(1 - \cos^2 \phi) \qquad (2)$$

The divisor of 4 compensates for the fact that this term is included for each of the four conformation angles ϕ around each link.

It is the parameter E_ϕ that we wish to determine. We will do this by assuming trial values for E_ϕ and minimizing the energy of the model with respect to the 11 structural variables. We concern ourselves only with the local minimum in the region of the experimental structure. All calculations were made with program WMIN,[24,25] which locates energy minima by search techniques or by Newton's method. Accelerated convergence algorithms[26] were used to ensure that the summations for both Coulomb and van der Waals energies gave values within 0.1 kcal/mol of convergence.

The results of these calculations are shown in Figure 2, in which the computed magnitudes of the average torsion angles ϕ_1, ϕ_2, and ϕ_3 are plotted against trial values of E_ϕ. It is clear that the choice of E_ϕ has a marked effect on the equilibrium torsion angles in the model structure. Also shown in Figure 2 are the observed values of the torsion angles and the values of E_ϕ that would have reproduced them exactly. Note that the calculated torsion-angle magnitudes are in a sequence that agrees with the observed values. This strengthens our conviction that the differences are the result of intermolecular interactions. A value of 8.68 kcal/mol for E_ϕ minimizes the sum of the absolute deviations of the observed and calculated ϕ's.

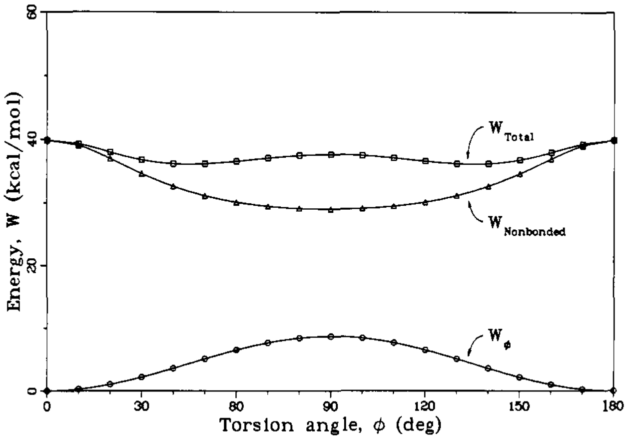

Figure 3. Contributions to the energy of an isolated molecule of 1,3,5-triphenylbenzene as one phenyl ring is turned about its ring–ring link. The other two phenyl groups are arbitrarily held in positions coplanar with the central ring.

Table I compares the observed and calculated parameters of the structure after adjusting the 11 variables using this best value of E_ϕ. The lattice parameters agree to within 2.9%; the rotation and translation of the molecule as a whole are only 0.6° and 0.03 Å, respectively; and the torsion angles are all within 1.1° of the values observed. This good agreement gives us confidence that our choice of nonbonded potential is reasonable and that the overall model is acceptable.

In order to gain a better understanding of the intramolecular torsion potential, we have made further calculations for the isolated molecule using the value of E_ϕ determined above. For this purpose we have idealized the geometry of the molecule so that each segment is planar, and chemically equivalent bond distances and angles are given their average values. Because we expect very little interaction between the three peripheral phenyl groups, we have arbitrarily held two of them in the plane of the central ring while one phenyl group is stepped through a full range of torsion angles. Figure 3 shows the contributions of nonbonded interactions and the π-bonding cosine potential to the overall molecular potential at 10° intervals. The cosine potential energy, W_ϕ, has minima at 0 and 180° and a maximum at 90°. The nonbonded interactions, $W_{\text{nonbonded}}$, on the other hand, have a minimum at 90° and maxima at 0 and 180°. The resulting overall potential, W_{total}, is relatively flat with minima at 44.2 and 135.8°. The net barriers to torsional rotation are only 3.7 and 1.5 kcal/mol at 0 and 90°, respectively.

Minimizing the energy of the isolated molecule with respect to torsion of all three phenyl groups produces a conformation with 3-fold symmetry, $\phi_1 = \phi_2 = \phi_3 = 43.6°$, and shows that the three phenyl groups are indeed almost independent. Going from the planar arrangement to the equilibrium conformation lowers the energy by 11.0 kcal/mol, slightly less than $11.1 = 3 \times 3.7$, where 3.7 kcal/mol is the energy change when only one phenyl group is allowed to turn. The distortions observed in the crystal tructure correspond to a total increase in intramolecular energy of only 0.8 kcal/mol. Clearly, strains of this magnitude can easily be accounted for by intermolecular interactions.

***p,p'*-Bitolyl.** The crystal structure[27] of this compound is monoclinic (space group $P2_1/c$) with eight molecules in the unit cell. Here, we are aided by the fortuitous circumstance that there are two crystallographically distinct molecules in the asymmetric unit, each in a general position so that its environment has no special symmetry. The torsion angles for the two kinds of molecules, again obtained by averaging the four conformation angles about each link, are −35.6 and 39.5°.

---

(24) Busing, W. R. *Acta Crystallogr., Sect. A* **1972**, *A28*, S252.

(25) Busing, W. R. "WMIN, A Computer Program to Model Molecules and Crystals in Terms of Potential-Energy Functions," ORNL-5747; Oak Ridge National Laboratory: Oak Ridge, TN, 1981.

(26) Williams, D. E. *Acta Crystallogr., Sect. A* **1971**, *A27*, 452–455.

(27) Casalone, G.; Mariani, C.; Mugnoli, A.; Simonetta, M. *Acta Crystallogr., Sect. B* **1969**, *B25*, 1741–1750.

Table II. *p,p'*-Bitolyl: Observed and Calculated Crystal Structure Parameters and Calculated Geometry of the Idealized Isolated Molecule[a, b]

	crystal				isolated molecule
	obsd[27]	calcd	calcd − obsd	%	calcd
a	9.77	9.66	−0.11	−1.1	
b	13.67	13.64	−0.03	−0.2	
c	18.25	17.54	−0.71	−3.9	
β	118.3	117.4	−0.9		
x_1	0.00	0.17	0.17		
θ_1	0.0	3.8	3.8		
ϕ_1	−35.6	−35.6	0.0		36.3
x_2	0.00	0.14	0.14		
θ_2	0.0	1.9	1.9		
ϕ_2	39.5	39.5	0.0		36.3

[a] $E_\phi = 11.44$ kcal/mol. [b] Units and notation as for Table I.

We treat each benzene ring and each methyl group as a rigid segment and permit three torsional degrees of freedom for each of the two molecules. Carbon atoms are given the experimental geometry, and hydrogen coordinates are calculated with the C–H bonds shortened, by 0.07 Å, to 1.020 Å for the benzenoid hydrogen atoms and 1.025 Å for those of the methyl groups. Each molecule is allowed six rotational and translational degrees of freedom in the crystal, and the four lattice parameters, a, b, c, and β, are adjusted, for a total of 22 structural variables in the model.

The potential functions used for the nonbonded interactions and ring–ring torsions are the same as those described above. No potential was included for the methyl group torsions except that arising from the nonbonded interactions. The first term of any such methyl torsion potential would be of the form cos 6ϕ, and we assume that it would be small compared to the ring–ring potential.

The energy was minimized using various torsion potentials, and Figure 4 shows the resulting torsion angles as a function of E_ϕ. Again, these angles depend strongly on this parameter. The observed angles are also indicated in the figure, and we see that both values are reproduced almost exactly for an E_ϕ of 11.44 kcal/mol.

Table II lists some observed and calculated parameters of the structure after adjusting the 22 variables using this best value of E_ϕ. The lattice translations agree to within 3.9%, the β angle changes by only 0.9°, the largest rotation and translation of the molecules are 3.8° and 0.17 Å, and the calculated mean phenyl–phenyl torsion angles are essentially the same as those observed. Again, the model seems reasonable, and the observed difference in the torsion angles of the two molecules is explained on the basis of intermolecular packing forces.

Only 8 of the 12 methyl hydrogen atoms were located in the X-ray study,[27] and we judge our calculated hydrogen positions to be better than those reported. We therefore make no comparison between the observed and calculated methyl torsion angles.

Williams' study of bitolyl[18] was similar to the present one, but the experimental lattice parameters were held constant and the methyl groups were rigidly fixed to the benzene rings. He represented the nonbonded interactions by a slightly different 6–exp potential[28] and found an E_ϕ of 9.0 kcal/mol, only a little smaller than our result. If the potential energy functions are realistic, then both methods should be capable of producing a good value of E_ϕ. The present procedure of adjusting all 22 structural parameters provides more assurance that these functions are, in fact, nearly correct.

Calculations were again made for the isolated molecule of *p,p'*-bitolyl with its geometry idealized as described above. The intramolecular potential curves are analogous to those of Figure 3 with energy minima at ϕ = 36.3 and 143.7°. The barriers to ring–ring rotation are 2.3 and 3.2 kcal/mol at 0 and 90°, respectively. Note that the larger value of E_ϕ causes the relative heights of these barriers to be reversed from those found for 1,3,5-triphenylbenzene. The phenyl–phenyl torsions observed in the crystal structure correspond to an increase in intramolecular energy of only 0.02 kcal for 1 mol of $C_{14}H_{14}$.

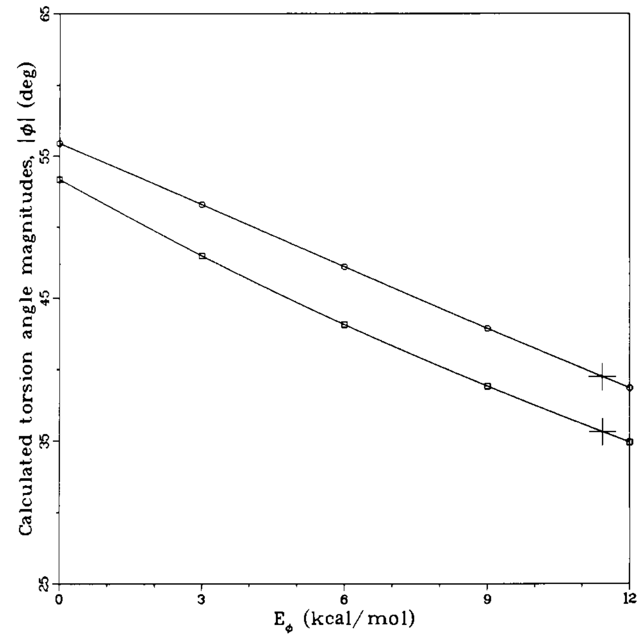

Figure 4. Magnitudes of the phenyl–phenyl torsion angles for the two nonequivalent molecules of *p,p'*-bitolyl obtained by minimizing the energy of a computational model of the crystal using various values of the π-bonding potential parameter E_ϕ. The + signs indicate the observed values of these angles.

The stable methyl orientation for this model has one hydrogen atom in a plane perpendicular to the ring, but the nonbonded interactions produce a barrier height of only 0.02 kcal/mol for each methyl group with a rotation of 30°. Thus, these rotations may be essentially free in the gas phase except at very low temperatures.

1,1'-Binaphthyl. This compound provides an especially good test of our procedure, because it crystallizes in two different forms with very different torsion angles. One of these forms is racemic with a crystal structure[29,30] that is monoclinic (space group $C2/c$) with four molecules per unit cell and a torsion angle, averaged as before, of 67.7°. The other form is chiral with a tetragonal structure[30,31] (space group $P4_32_12$) with four molecules per unit cell and a torsion angle of 101.4°. In each case, the torsion angle of the planar syn conformation is defined as zero.

In both of these structures, each binaphthyl molecule is situated on a crystallographic twofold axis passing through the center of the naphthyl–naphthyl link. This axis is perpendicular to the link and relates the two naphthyl groups to each other.

Each naphthyl moiety was treated as a rigid group. The hydrogen positions were calculated as before with C–H bonds foreshortened to 1.020 Å. The seven structural variables for the monoclinic form are the four lattice parameters a, b, c, and β, one translation of the molecule along the twofold axis, one rotation of the molecule about this axis, and the naphthyl–naphthyl torsion angle. The five variables for the tetragonal form include the lattice parameters a and c (with b constrained to equal a), one molecular rotation, one translation, and one torsion angle. The form of the potential was the same as that used above.

The energies of these models were minimized using several trial values of E_ϕ, and Figure 5 shows the values of the torsion angles ϕ for both crystal forms as a function of this parameter. The effect of E_ϕ on the calculated ϕ values is considerably less for 1,1'-bi-

---

(28) Williams, D. E. *Trans. Am. Crystallogr. Assoc.* **1970**, *6*, 21–33.

(29) Kerr, K. A.; Robertson, J. M. *J. Chem. Soc., B* **1969**, 1146–1149.

(30) Kress, R. B.; Duesler, E. N.; Etter, M. C.; Paul, I. C.; Curtin, D. Y. *J. Am. Chem. Soc.* **1980**, *102*, 7709–7714.

(31) Kuroda, R.; Mason, S. F. *J. Chem. Soc., Perkin Trans. 2* **1981**, 167–170.

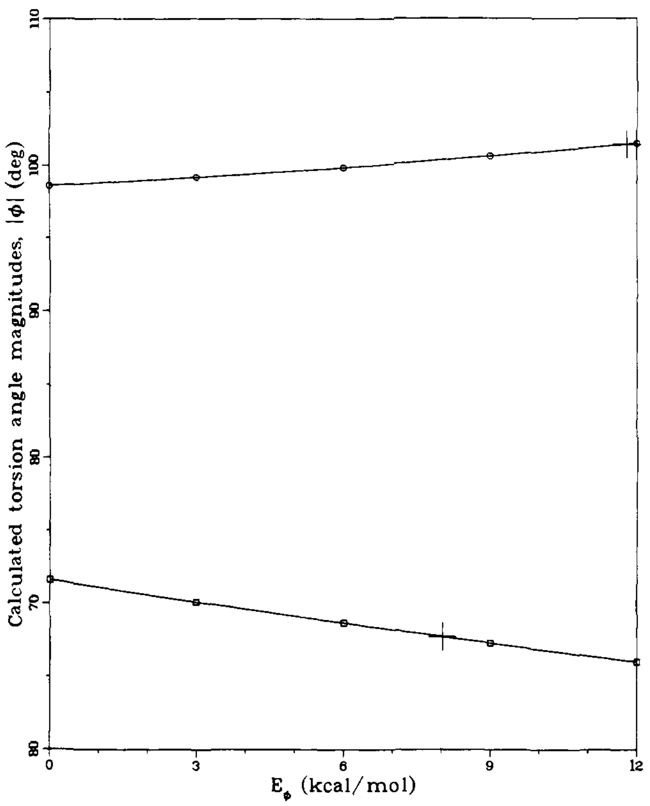

Figure 5. Magnitudes of the naphthyl–naphthyl torsion angles of 1,1′-binaphthyl obtained by minimizing the energies of computational models of the two crystalline forms using various values of the π-bonding potential parameter E_ϕ. The squares represent the racemic form and the circles the chiral form. The + signs indicate the observed values of these angles.

Table III. 1,1′-Binaphthyl: Observed and Calculated Crystal Structure Parameters for the Racemic and Chiral Forms and Calculated Geometry of the Isolated Molecule[a,b]

	crystal				isolated molecule
	obsd	calcd	calcd – obsd	%	calcd
		Racemic[29]			
a	20.98	21.01	0.03	0.1	
b	6.35	6.25	−0.10	−1.6	
c	10.13	10.27	0.14	1.4	
β	105.2	106.4	1.2		
x	0.00	0.03	0.03		
θ	0.0	0.6	0.6		
ϕ	67.7	67.0	−0.7		78.4
		Chiral[30]			
a	7.18	7.09	−0.09	−1.3	
c	27.68	28.04	0.36	1.3	
x	0.00	0.00	0.00		
θ	0.0	0.7	0.7		
ϕ	101.4	100.8	−0.6		78.4

[a] E_ϕ = 9.52 kcal/mol. [b] Units and notation as for Table I.

naphthyl than for the two compounds discussed above. A compromise value of E_ϕ of 9.52 kcal/mol reproduces the angles in both forms to within 0.7°. Table III shows the observed and calculated parameters for each structure, which are again in good agreement. After minimization, the calculated energy of the racemic crystal is 1.6 kcal/mol lower than that of the chiral form. It appears, therefore, that if the zero-point energies are comparable, the racemic crystal is the stable form at 0 K.

Calculations for the idealized isolated molecule, using the compromise value for E_ϕ, are plotted in Figure 6. Again, an angle of 0° represents the planar syn configuration and 180° the planar anti conformation. At either of these two barrier positions, the hydrogen–hydrogen contacts would be much shorter than in the compounds discussed previously, so the energy rises very steeply toward these extremes. It is the existence of these high barriers, of course, that permits this compound to be resolved into its chiral forms.

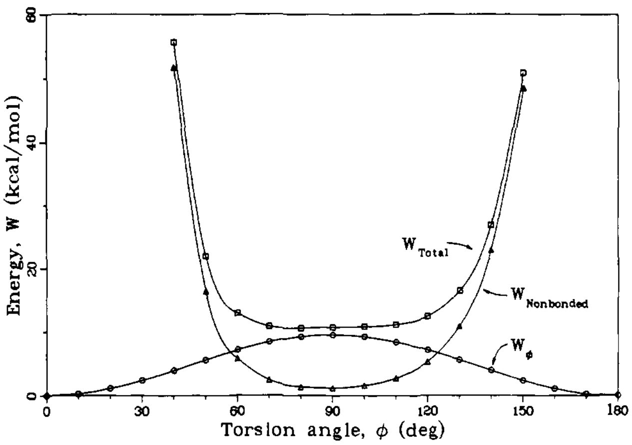

Figure 6. Contributions to the energy of an isolated molecule of 1,1′-binaphthyl as rigid planar naphthyl groups are turned about their link. The 0° position represents the planar syn conformation.

The cosine torsion potential is not sufficient to produce a double minimum in the net potential. Instead, it produces a very flat-bottomed well with a minimum at 78.4°. It is this flat-bottomed well that permits crystal forces to distort the torsion angles to the widely separated values found in the two crystal forms. The intramolecular energy increases by only 0.5 or 0.3 kcal/mol in going from the isolated molecule to the monoclinic crystal or the tetragonal crystal, respectively.

The potential curve of Figure 6 is qualitatively similar to that computed by Carter and Liljefors[32] using the force field of Wertz and Allinger.[33] Although our one-parameter model with rigid naphthyl groups produces a potential that rises too steeply toward the barriers, we believe that its shape in the middle region can be accepted as derived from the observed crystal structures.

***o*-Terphenyl.** The crystal structure of *o*-terphenyl is known from neutron diffraction work[34] and from an independent X-ray diffraction study.[35] The orthorhombic space group is $P2_12_12_1$, and there are four molecules in the unit cell. Each molecule is in a general position so that no special symmetry is imposed by its environment. The two torsion angles, averaged as described above, are ϕ_1 = 42.4 and ϕ_2 = 62.0°.

Our initial model has three segments similar to those used above. Each benzene ring is treated as rigid with carbon atoms in the geometry found by neutron diffraction. Because hydrogen atom positions are well determined by neutron diffraction, we start with the experimental hydrogen locations and foreshorten each C–H bond by 0.070 Å to satisfy the requirements of the nonbonded potential. The structural variables are the two intramolecular torsions, six rotations and translations of the molecule as a whole, and the three lattice parameters, for a total of 11 degrees of freedom. The potential is again taken as that described above.

Figure 7 shows the calculated values of ϕ as a function of E_ϕ, and the best compromise value of E_ϕ is selected to be 9.28 kcal/mol. Table IV lists values of some observed and calculated structural parameters using this potential for the three-segment model. The agreement is seen to be reasonable, although the discrepancies for the two torsion angles are larger than those found for 1,3,5-triphenylbenzene or *p,p*′-bitolyl. This may be an indication that the cosine form of the torsion potential is not the best choice. Modification of this form would have the greatest effect

---

(32) Carter, R. E.; Liljefors, T. *Tetrahedron* **1976**, *32*, 2915–2922.

(33) Wertz, D. H.; Allinger, N. L. *Tetrahedron* **1974**, *30*, 1579–1586.

(34) Brown, G. M.; Levy, H. A. *Acta Crystallogr., Sect. B* **1979**, *B35*, 785–788.

(35) Aikawa, S.; Maruyama, Y.; Ohashi, Y.; Sasada, Y. *Acta Crystallogr., Sect. B* **1978**, *B34*, 2901–2904.

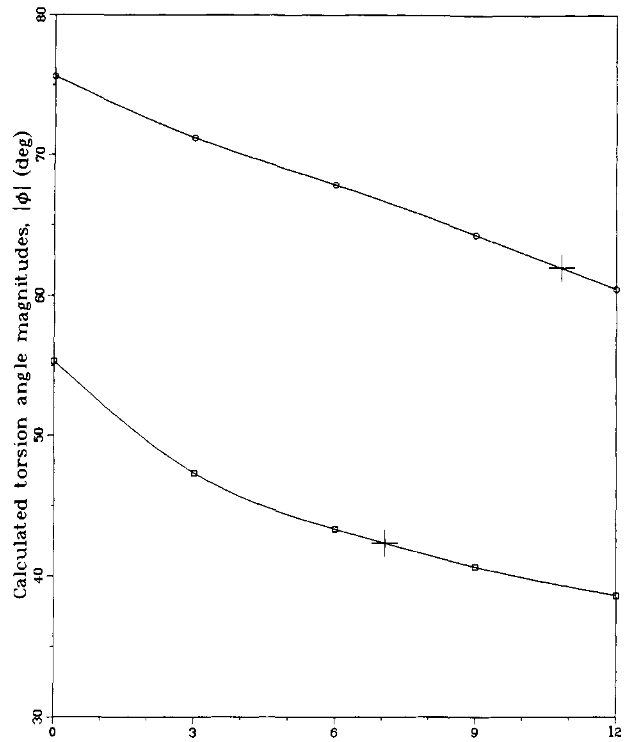

Figure 7. Magnitudes of the phenyl–phenyl torsion angles in *o*-terphenyl obtained by minimizing the energy of a computational model of the crystal using various values of the π-bonding potential parameter E_ϕ. The molecule was represented by a three-segment model. The + signs indicate the observed values of the angles.

Table IV. *o*-Terphenyl: Observed and Calculated Crystal Structure Parameters and Calculated Geometry of the Idealized Isolated Molecule[a, b]

		crystal						isolated molecule
		three-segment model			five-segment model			
	obsd[34]	calcd	calcd − obsd	%	calcd	calcd − obsd	%	calcd
a	18.58	18.61	0.03	0.2	18.63	0.05	0.3	
b	6.02	5.89	−0.13	−2.2	5.91	−0.11	−1.8	
c	11.73	11.46	−0.27	−2.3	11.40	−0.33	−2.8	
x	0.00	0.05	0.05		0.03	0.03		
θ	0.0	2.2	2.2		1.8	1.8		
ϕ_1	42.4	40.3	−2.1		40.7	−1.7		54.3
ϕ_2	62.0	63.8	1.8		63.6	1.6		54.3
ψ	5.2				5.2	0.0		2.5
α_1	123.6				123.5	−0.1		122.9
α_2	123.0				123.2	0.2		122.9

[a] E_ϕ = 9.28 kcal/mol, E_ψ = 41.6 kcal/mol, k_α = 0.94 mdyn Å/rad^2. [b] Units and notation as for Table I.

for compounds such as *o*-terphenyl that are observed to have large differences between the individual torsion angles.

The crystal structure of *o*-terphenyl also shows two other kinds of strains that arise from the strong intramolecular interaction between the two peripheral phenyl groups, and these are shown in Figure 8. The bond angles 1–1′–2′ and 1″–2′–1′ (designated α_1 and α_2) are 123.6 and 123.0°, respectively, while angles 1–1′–6′ and 1″–2′–3′ are reduced correspondingly to 118.4 and 117.4°. Furthermore, the ring–ring links are forced out of the plane of the central ring so that the torsion angle 1–1′–2′–1″ (designated as ψ) is 5.2°.

We proceed to model these distortions by dividing the molecule into five segments as follows. Let the central ring with its hydrogen atoms be the basic rigid segment. Attach to it the two links 1′–1 and 2′–1″ of fixed length, which pivot on atoms 1′ and 2′, with two degrees of freedom each. The two rigid phenyl groups then pivot on atoms 1 and 1″, with three degrees of freedom each. The structural variables include these ten internal degrees of freedom, the six molecular rotations and translations, and the three unit-cell edges, for a total of 19 adjustable parameters.

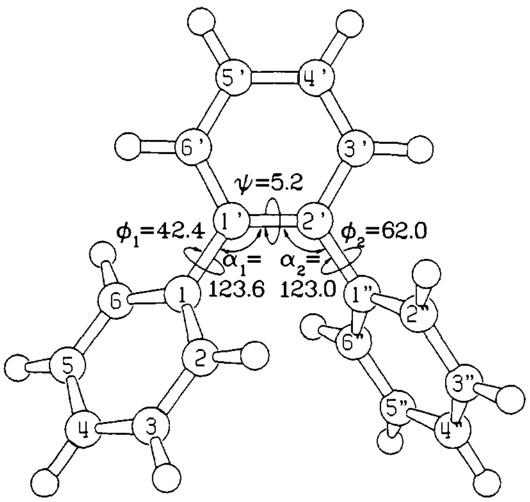

Figure 8. Molecular geometry of *o*-terphenyl as observed in the crystal structure. Each angle ϕ is the average of four conformation angles as described in the text. The angle ψ is the conformation angle 1–1′–2′–1″. The α's are the bond angles indicated. All angles are in degrees.

With this more flexible model, we need additional terms in the intramolecular potential. We introduce a quadratic bond angle distortion term of the form

$$V(\alpha) = (k_\alpha/2)(\alpha - 120°)^2 \qquad (3)$$

where k_α is a force constant. This expression generates a contribution for each of the eight variable ring–link angles and tends to equalize the pairs of angles on each side of a link.

We also need terms in the potential that will tend to keep a link in the plane of the ring to which it is attached. For this purpose, we include a π-bonding cosine potential (eq 4) for each

$$V(\psi) = (E_\psi/4)(1 - \cos^2 \psi) \qquad (4)$$

of the four torsion angles about each ring bond that is adjacent to a link. There are seven such ring bonds (1–2, 1–6, 1′–2′, 2′–3′, 1′–6′, 1″–2″, and 1″–6″ in Figure 8), so that eq 4 introduces 28 terms in the potential.

The values of k_α and E_ψ were adjusted by trial using the value of E_ϕ determined earlier, so that, when the energy was minimized with respect to the 19 structural variables, the experimental bond angles α_1 and α_2 and the torsion angle ψ were reproduced as well as possible. A value of 0.94 mdyn Å/rad^2 was obtained for k_α, much larger than the value 0.40 mdyn Å/rad^2 recommended by Kao and Allinger.[36] (Or course, the values are not required to agree, since these authors use a quite different nonbonded potential.) The value of E_ψ is 41.6 kcal/mol, considerably larger than our value for E_ϕ indicating, as expected, that the tendency for ring–link planarity is much stronger than that for ring–ring planarity. The overall agreement of the observed and calculated structural parameters for the five-segment model is also presented in Table IV.

To understand the potential of the isolated molecule, we have again idealized the geometry by averaging chemically equivalent distances and angles and by requiring the segments to be planar. Minimizing the energy of the five-segment isolated molecule with respect to the ten internal variables yields a geometry also described in Table IV. Note that the predicted configuration has twofold symmetry, with $\phi_1 = \phi_2$ = 54.3°. The link–link torsion angle ψ has a magnitude of 2.5°, somewhat smaller than the 5.2° found in the crystal. Examination of the crystal structure shows that molecules may be forced together in a way that wedges the two phenyl rings apart, accounting for this difference. The

---

[36] Kao, J.; Allinger, N. L. *J. Am. Chem. Soc.* **1977**, *99*, 975–986.

Table V. Parameters of Four Published Potentials Expressed in the Form of Eq 5[a]

	Williams and Starr[9]	Mirsky[10]	Ermer and Lifson[11]	Wertz and Allinger[13]
		C–C		
A	577.139	421.0	943.000	171.151 5
B	87 802.1	71 600.0	27 372.1	164 913.9
C	3.60	3.68	0	0
n	0	0	9	12
		H–H		
A	32.514 9	29.0	28.295	103.673 9
B	2 791.7	4 900.0	903.771	25 068.9
C	3.74	4.29	0	0
n	0	0	9	12
		C–H		
A	136.987 6	118.0	163.472	105.657 0
B	15 656.2	18 600.00	4 979.44	48 602.6
C	3.67	3.94[b]	0	0
n	0	0	9	12
ΔA_{CH}[c]	0	7.506	0.125	−27.549 0
rule for r_{CH}	$r' = r - 0.07$	$r' = r$	$r' = r$	$r' = 0.9r$
benzenoid r'[d]	1.020	1.080[e]	1.090	0.9810
methyl r'[f]	1.025	1.095	1.095	0.9855
charge benzenoid q_H	0.1530	0	0	0
methyl q_H	0.0765	0	0	0

[a] Energy in kcal/mol, distance in angstroms, charge in electrons. [b] A typographical error in ref 10 has been corrected. [c] $\Delta A_{CH} = A_{CH} - (A_{CC}A_{HH})^{1/2}$. [d] The value 1.090 is the mean C–H distance found in *o*-terphenyl by neutron diffraction.[34] [e] This is the value used by Mirsky (personal communication). [f] The value 1.095 is the C–H distance in ethane.[38]

link–ring bond angles α of the isolated molecule are not changed much from their values in the crystal.

The potential of the isolated molecule has been further explored by forcing the ring–ring torsion angles to take on various values and allowing the other eight internal variables to relax. Figure 9 shows the resulting energies as a function of $\phi = \phi_1 = \phi_2$. Also plotted are the torsion angle ψ and the bond angles $\alpha = \alpha_1$ and α_2, which describe the model for various values of ϕ. It can be seen that these angles become severely strained as ϕ approaches 0 or 180°. It is clear that our model, which assumes rigid benzene rings, is not likely to be realistic for ϕ values approaching these extremes. On the other hand, these distortions are relatively small in the range of ϕ from 40° to 140°, so that near the experimental geometry, the model appears to be reasonable.

In Figure 9, the curve labeled W_ϕ is the ring–ring cosine potential, which goes through a maximum of $2E_\phi$ at 90°. Also shown is the curve $W_\phi + W_\psi + W_\alpha$, which includes the additional energy terms $V(\alpha)$ and $V(\psi)$ from eq 3 and 4. These terms make appreciable contributions when the torsion angles are forced toward 0 or 180°. The curve for $W_{\text{nonbonded}}$ shows a minimum at 90°, as expected, and W_{total} has a barrier of only 2.7 kcal/mol at this geometry. The distortions observed in the crystal structure correspond to a calculated internal energy 0.8 kcal/mol higher than that of the gas-phase molecule.

Conclusions

We have shown that when an observed crystal structure contains a molecule distorted either by intermolecular packing forces or by nonbonded intramolecular forces and when these forces can be assumed to be known, then the constants of the intramolecular potentials that balance these forces can be determined. In this way we have obtained the phenyl–phenyl conjugation energy constant E_ϕ for four molecules in five crystal structures and found values ranging from 8.68 to 11.44 kcal/mol. These constants tend to be somewhat higher than the values obtained from some theoretical calculations of this coefficient for biphenyl. Fischer-Hjalmars[14] found a value of 6.23 kcal/mol from a Pariser–Parr–Pople calculation; Casalone, Mariani, Mugnoli, and Simonetta[15] obtained about 7.6 kcal/mol by the Hückel method; and Dewar and Harget[16] calculated 8.87 kcal/mol by using a self-consistent-field molecular orbital approach.

On the other hand, Almlöf[17] has made an MO LCAO calculation for biphenyl using a Gaussian basis set of double-ζ quality, which yields a torsion barrier at 90° of 4.5 kcal/mol, much larger than the 1.5 or 3.2 kcal/mol that we obtain for 1,3,5-triphenylbenzene or *p,p'*-bitolyl, respectively. Although he did not separate out the conjugation energy in this calculation, the implication is that it is larger than that from our determination.

Perhaps some of the discrepancies among the several values that we have deduced from experiment may be attributed to real chemical differences in the species considered. However, the large differences between the values predicted for the two forms of 1,1′-binaphthyl (Figure 5) or for the two angles in *o*-terphenyl (Figure 7) seem to indicate that these discrepancies arise mostly from errors in the assumed form of the potential. We hope that by using potentials of more complexity the consistency of the results will be improved.

Appendix

Selecting a Nonbonded Potential. The procedure described above depends completely on our being able to describe the nonbonded intermolecular interactions realistically. Tests of proposed potential-energy functions can be made by incorporating them into model crystals, minimizing the energy with respect to the structural variables, and comparing the observed and calculated crystal structure parameters, heats of sublimation, or frequencies of external vibrational modes. Recently, procedures have been described[37] for testing a potential function by using a simple Monte-Carlo method to calculate various thermodynamic properties of a crystal for comparison with experiment. For the present purposes, however, we limit our tests to a comparison of observed and calculated crystal structures.

Of the many hydrocarbon potentials in the literature, we have selected four for comparison. We have resisted the temptation to "improve" these potentials to produce better agreement for the crystals of interest. All of them should be universally applicable, since they are based on the properties of many compounds (but not the five structures studied here). The four potentials can be described in the universal notation,[10]

$$V(r) = -A_{ij}r^{-6} + B_{ij}r^{-n}\exp(-C_{ij}r) + q_iq_jr^{-1} \qquad (5)$$

and their parameters are listed in Table V. Because most of these parameters have been computed from values published in different forms and different units, we present the numbers actually used in our calculations to six significant digits.

---

(37) Pertsin, A. J.; Ivanov, Y. P.; Kitaigorodsky, A. I. *Acta Crystallogr., Sect. A* **1981**, *A37*, 908–913.

(38) Shaw, D. E.; Lepard, D. W.; Welsh, H. L. *J. Chem. Phys.* **1965**, *42*, 3736–3737.

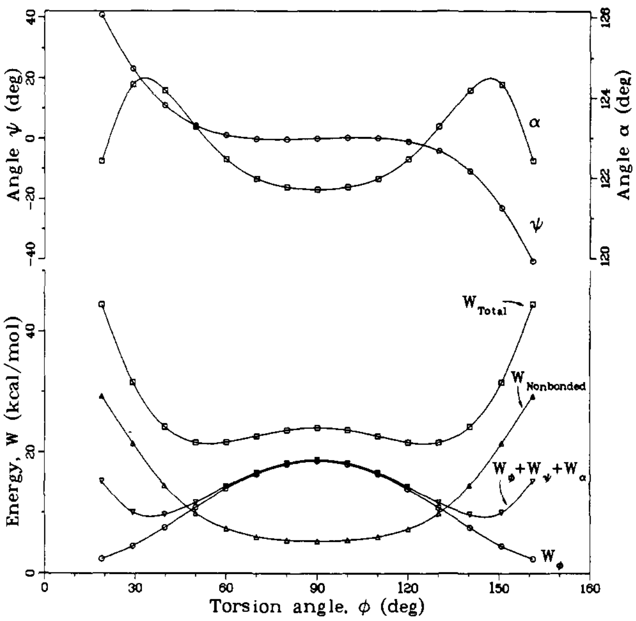

Figure 9. Contributions to the energy of an isolated molecule of *o*-terphenyl as the two phenyl rings are turned cooperatively through equal torsion angles. For each setting of the angles ϕ, the five-segment model was allowed to relax. The resulting values of ψ and α (see Figure 8) are also plotted.

The 6–exp–1 potential of Williams and Starr[9] is their potential II, based on the reported crystal structures of 18 hydrocarbons, both aromatic and aliphatic. They used the heats of sublimation of benzene and *n*-hexane to scale the potentials. This is the only potential of the four that includes Coulomb interactions.

Mirsky[10] recommends 6–exp potentials that were fitted to crystal structure, heat-of-sublimation, and elasticity data. The basis crystal structures were extrapolated to absolute zero when possible, and for this reason, we are not surprised to find that these potentials predict lattice parameters smaller than our room-temperature values.

Ermer and Lifson[11] reported their 6–9 nonbonded potential as part of a general molecular force field optimized to fit 259 vibrational frequencies, 44 conformational data, and 10 thermochemical quantities. These data involved 19 different hydrocarbon molecules, but no crystal packing information was used.

Wertz and Allinger[13] describe a revised force field that includes a 6–12 nonbonded interaction term. The parameters of this force field were optimized to fit 25 distances, angles, and torsion angles and 53 heats of formation for hydrocarbon molecules. Also included as an observation was a single intermolecular packing distance for crystalline *n*-hexane.

Williams' method[26] for the accelerated convergence of lattice sums assumes that $A_{CH} = (A_{CC}A_{HH})^{1/2}$, but three of the four potentials tested do not satisfy this condition. In these cases, correction terms of the form $-\Delta A_{CH}r^{-6}$ were added to the direct lattice sums to ensure the calculation of the correct energy to within 0.1 kcal/mol.

In setting up the models, we again used calculated hydrogen atom positions, except for the *o*-terphenyl structure, where the positions are known from neutron diffraction. Care was taken to foreshorten the C–H distances when the definition of the potential required it. Table V lists the rules for the foreshortening as well as the C–H distances used in each case for the X-ray structures.

Tests were made by minimizing the energy of the model crystal with respect to the lattice parameters and the translation and rotation of the molecule as a whole. In general, the molecule was held rigid with its experimental geometry, since this is the geometry our model would have if we were able to reproduce the intramolecular potential exactly. For tests on bitolyl, the methyl groups were permitted rotational freedom, because the correct methyl orientation is not known experimentally.

Table VI. Discrepancies Between Observed and Calculated Structures for Five Crystals using Four Different Nonbonded Potentials in Rigid-Molecule Packing[a]

potential	Williams and Starr[9]	Mirsky[10]	Ermer and Lifson[11]	Wertz and Allinger[13]
	1,3,5-Triphenylbenzene			
Δa	−2.9	−5.7	−9.5	−11.2
Δb	0.2	−1.1	0.1	0.0
Δc	−0.4	−1.9	−0.4	−0.5
Δx	0.03	0.08	0.10	0.07
$\Delta\theta$	0.7	0.9	1.5	2.1
	p,p'-Bitolyl			
Δa	−1.1	−3.5	−3.0	−6.5
Δb	−0.2	−1.4	−0.2	−1.1
Δc	−3.9	−10.0	−10.5	−10.1
$\Delta\beta$	−0.9	−3.4	−3.7	−2.9
Δx_1	0.17	0.28	0.24	0.19
$\Delta\theta_1$	3.7	11.1	6.9	5.2
Δx_2	0.14	0.21	0.19	0.12
$\Delta\theta_2$	1.9	7.0	5.3	2.4
	1,1'-Binaphthyl (Racemic)			
Δa	0.1	−1.8	−0.2	0.1
Δb	−2.0	−6.0	−6.3	−5.1
Δc	1.9	0.4	−0.4	−1.8
$\Delta\beta$	1.1	−0.2	1.0	2.2
Δx	0.03	0.08	0.09	0.07
$\Delta\theta$	0.6	1.0	0.9	0.8
	1,1'-Binaphthyl (Chiral)			
Δa	−1.3	−3.6	−3.3	−4.2
Δc	1.5	1.7	1.1	1.3
Δx	0.01	0.02	0.04	0.15
$\Delta\theta$	0.8	1.2	1.1	1.9
	o-Terphenyl			
Δa	−0.3	−2.0	−1.3	−1.2
Δb	−0.9	−3.5	−4.1	−4.6
Δc	−2.6	−3.8	−4.6	−6.0
Δx	0.06	0.09	0.13	0.17
$\Delta\theta$	1.7	1.5	2.3	3.0
	Summary			
$\overline{\lvert\Delta a, \Delta b, \Delta c\rvert}$	1.4	3.3	3.2	3.8
$\overline{\lvert\Delta\beta\rvert}$	1.0	1.8	2.3	2.6
$\overline{\Delta x}$	0.07	0.13	0.13	0.13
$\overline{\Delta\theta}$	1.6	3.8	3.0	2.6

[a] Δa, Δb, and Δc are lattice parameter differences (%); $\Delta\beta$ is lattice angle change (deg); Δx is molecular translation (Å); $\Delta\theta$ is molecular rotation (deg).

Table VI lists the differences between observed and calculated lattice parameters and the rotations and translations of the rigid molecules for the five crystalline substances for each of the four nonbonded potentials. The table also summarizes the discrepancies as averages over the substances. The averages make it clear that the potential of Williams and Starr performs consistently better than the other three in reproducing the experimental structures. Its superiority over the potential of Mirsky may arise from the temperature effect mentioned above, or it may be the result of adding one more parameter, the Coulomb charge separation, to the fit. The other two potentials were not developed primarily to reproduce crystal structures, so it is not surprising that they are inferior to the potential of Williams and Starr in this respect. Whether a force field based on the Williams and Starr potential can reproduce heats of formation and other molecular properties remains to be tested. We believe, however, that it is the most appropriate potential for the present purposes.

Registry No. 1,3,5-Triphenylbenzene, 612-71-5; *p,p'*-bitolyl, 613-33-2; 1,1'-binaphthyl, 604-53-5; *o*-terphenyl, 84-15-1.